ISSN 0006-2979, Biochemistry (Moscow), 2012, Vol. 77, No. 8, pp. 896-900. © Pleiades Publishing, Ltd., 2012.
Published in Russian in Biokhimiya, 2012, Vol. 77, No. 8, pp. 1089-1094.

Domain Motions of Class I Release Factor Induced by Binding with Class II Release Factor from *Euplotes octocarinatus*

Jie Chen[1], Bing-sheng Yang[2], and Ai-hua Liang[1]*

[1]*Institute of Biotechnology and* [2]*Institute of Molecular Science, Key Laboratory of Chemical Biology and Molecular Engineering of Ministry of Education, Shanxi University, Taiyuan 030006, China; fax: 0086-351-7011499; E-mail: aliang@sxu.edu.cn*

Received February 19, 2012
Revision received March 12, 2012

Abstract—The binding of both factors (eRF1 and eRF3) is essential for fast kinetics of the termination of protein translation. The C-terminal domain of eRF1 is known to interact with the C domain of eRF3. Eo-eRF1b contains two highly conserved tryptophan residues (W-11 and W-373), W-11 located in the Eo-eRF1b N domain and W-373 located in the Eo-eRF1b C domain. Fluorimetry was used to study the interactions of the proteins. When binding with Eo-eRF3Cm6, the emission peak of Eo-eRF1b is blue shifted, while the emission peak of Eo-eRF1bC has no notable change. Our results suggest that the eRF1–eRF3 interaction induces the N and C domain of eRF1b to become closer to each other.

DOI: 10.1134/S000629791208010X

Key words: steady-state fluorescence quenching, eRF1–eRF3 interaction, *Euplotes octocarinatus*

Termination of protein synthesis is triggered by the appearance of one of three stop codons (UAA, UGA, and UAG) in the decoding center of the small ribosomal subunit. In eukaryotes, this process is governed by two classes of peptide release factors, eRF1 and eRF3. eRF1 recognizes the stop codon and promotes nascent peptide chain release, while eRF3 facilitates this process via its interaction with eRF1 [1]. eRF1 proteins from eukaryotic species share significant homology at the primary amino acid sequence level. The human eRF1 structure, in a crystal structure [2] and in solution [3], consists of three domains (N, M, and C domains) that correlate with its three different functions. The N domain is implicated in stop codon recognition [3-5]. The tip of the M domain contains the invariant GGQ motif in both eukaryotic and prokaryotic RFs, which is required to trigger peptidyl-tRNA hydrolysis in eukaryotes [6, 7]. The C domain of eRF1 interacts with the C domain of eRF3 [8-11].

The binding complex of both factors, which appears to cause conformational changes in one or both factors, is essential for fast kinetics of the termination of translation [12-15]. It was found that the N domain of human eRF1 is not involved in interaction with eRF3, whereas the MC domain binds as efficiently as the whole eRF1 molecule and induces GTP binding to eRF3 and GTPase activity of the eRF3–ribosome complex [14]. Hatin's results showed that some mutations in the M or/and C domain of eRF1 could also affect termination [16]. Mutations in the TASNIKS motif, which is highly conserved in the eRF1 N domain, eliminated the eRF3 requirement for peptide release at UAA and UAG codons, but not UGA codons. These results suggest that the TASNIKS motif and eRF3 function together to trigger eRF1 conformational changes [13]. A new question arises, how the TASNIKS motif in eRF1 N domain and eRF3 function together triggering eRF1 conformational changes. To better understand the likely mechanisms of the interaction between eRF1 and eRF3, we studied conformational changes in eRF1 due to binding with eRF3 by fluorescence spectroscopy. As reported before for *Euplotes octocarinatus*, a kind of ciliated protozoan, it has two genes encoding class I RFs: Eo-eRF1a and Eo-eRF1b [17],

Abbreviations: eRF1, class I polypeptide release factor in eukaryotes; eRF3, class II polypeptide release factor in eukaryotes; Eo-eRF1b, class I polypeptide release factor b in *Euplotes octocarinatus*; Eo-eRF1bN, N domain of Eo-eRF1b; Eo-eRF1bC, C domain of Eo-eRF1b; Eo-eRF3, class II polypeptide release factor in *E. octocarinatus*; Eo-eRF3Cm6, truncated peptide of Eo-eRF3 (a.a. 640-723); Eo-eRF1b·Eo-eRF3Cm6, heterodimeric complex of Eo-eRF1b and Eo-eRF3Cm6; Eo-eRF1bC·Eo-eRF3Cm6, heterodimeric complex of Eo-eRF1bC and Eo-eRF3Cm6.

* To whom correspondence should be addressed.

which are 79% identical in sequence. The interaction between eRF1a and eRF3 of *E. octocarinatus* has been confirmed *in vivo* and *in vitro* [18]. It was shown that a short portion of the C-terminal domain of eRF3 (Eo-eRF3Cm6) was sufficient for eRF1a binding in *E. octocarinatus* [18]. Later we found that the expression level of Eo-eRF1b was much higher than that of Eo-eRF1a [19]. In this study, the interaction between Eo-eRF1bC and Eo-eRF3Cm6 was confirmed by pull-down and Western blot assays. Then the conformational changes in Eo-eRF1b due to the protein interaction were monitored by fluorescence spectroscopy.

MATERIALS AND METHODS

Plasmid constructs. The *E. octocarinatus eRF1b* gene contains three UGA (297, 384, and 1125) stop codons that are reassigned for cysteine [17, 20]. UGA 297 and UGA 384 are located in its N domain, while UGA 1125 is located in its C domain. To express the *Eo-eRF1b* gene in *Escherichia coli*, these UGAs (297, 384, and 1125) were mutated to the standard cysteine code UGT. Site-directed mutagenesis was carried out using the TaKaRa Mutant Best kit (TaKaRa Biotechnology Co., China). Plasmids pRSETC-Eo-eRF1b (a.a. 1-437), pRSETC-Eo-eRF1bN (a.a. 1-140), and pRSETC-Eo-eRF1bC (a.a. 274-437) were constructed by insertion of an *Nhe*I/*Xho*I digested PCR product into the same sites of pRSETC (Invitrogen, USA). The PCR products were amplified by the proper primers and plasmid Te-Eo-eRF1b [17].

Protein expression, purification, and *in vitro* pull-down analysis. The plasmids pRSETC-Eo-eRF1b (a.a. 1-437), pRSETC-Eo-eRF1bN (a.a. 1-140), and pRSETC-Eo-eRF1bC (a.a. 274-437) were transformed into strain *E. coli* BL21(DE3). Transformants were grown to an OD_{600} value of 0.4-0.6 at 37°C and induced with 0.1 mM isopropyl-1-thio-β-D-galactoside (IPTG) for 10 h at 25°C. Cells were harvested, lysed by sonication on ice, and centrifuged at 12,000*g* for 15 min. The supernatant containing soluble recombinant protein was saved for purification. Purification of recombinant proteins and Western blot analysis were carried out as previously described [21] with minor modifications. Eo-eRF3Cm6, a truncated peptide of Eo-eRF3 (a.a. 640-723), was previously verified sufficient for eRF1a binding in *E. octocarinatus* in our laboratory. To carry out pull-down analysis *in vitro*, Eo-eRF3Cm6 carries a GST tag (GST–Eo-eRF3Cm6) different from Eo-eRF1bC. The same conditions and protocols were used for transformation, growth, and induction with the plasmid pGEX-6p1-eRF3cm6 (a.a. 640-723) [18]. *In vitro* pull-down analysis was carried out as previously described [18] with minor modifications.

Fluorescence spectroscopy. Steady-state fluorescence of protein solutions were recorded using a F-2500 fluorescence spectrophotometer with fast scan speed and low sensitivity. Emission spectra were recorded from 300 to 450 nm. The slit width was kept at 10 nm in excitation and emission measurements. Additionally, only tryptophan is excited at 295 nm [22]. Therefore, the excitation wavelength of 295 nm was used for subsequent analysis of the proteins. Fluorescence single quenching measurements were as described previously [23] with minor modifications. The Stern–Volmer equation was taken as: $F_0/F = 1 + K_{SV}[Q]$.

The modified Stern–Volmer equation was taken as: $F_0/\Delta F = 1/(K_{SV} \cdot f_a \cdot [Q]) + 1/f_a$, where F_0 is initial fluorescence intensity; F is the total fluorescence intensity in the presence of quencher; ΔF is quenchable fluorescence intensity; f_a is the fraction of the initial fluorescence that is accessible to the quencher Q; K_{SV} is the Stern–Volmer constant of quencher Q. The plot of $F_0/\Delta F$ vs. $1/[Q]$ results in a straight line.

RESULTS

Protein expression, purification, and *in vitro* pull-down. The fusion proteins Eo-eRF1b-6×His, Eo-eRF1bN-6×His, and Eo-eRF1bC-6×His were expressed in *E. coli* BL21(DE3) and purified by affinity chromatography using Ni-NTA-agarose. To test whether the fusion proteins could bind to the eRF3Cm6 protein of *E. octocarinatus*, pull-down analysis was carried out. The GST–Eo-eRF3Cm6 fusion protein was first immobilized onto glutathione Sepharose 4B beads, followed by incubation with the fusion protein sample. After washing the bead mixture with binding buffer to remove the non-specifically binding proteins, the protein complex was eluted with glutathione and analyzed by Western blot with an anti-His tag probe (Fig. 1). The result indicated that immobilized GST–Eo-eRF3Cm6 could form a specific complex with Eo-eRF1b and Eo-eRF1bC from supernatant, while Eo-eRF1bN could not bind with Eo-eRF3Cm6. Our results are identical to the previous conclusions from Kononenko and colleagues by isothermal titration calorimetry [14]. These purified complexes without GST tag were used in the subsequent fluorescence spectroscopy analysis.

Fluorescence spectroscopy. Eo-eRF1b contains two highly conserved tryptophan residues (W-11 and W-373), W-11 located in Eo-eRF1bN and W-373 located in Eo-eRF1bC. Excitation of Eo-eRF1b, Eo-eRF1bN, and Eo-eRF1bC at given wavelengths resulted in emission spectra with a maximum at 340, 345, and 336 nm, respectively (Fig. 2). So the two tryptophans have different local environment, the local environment of tryptophan in Eo-eRF1bC being more hydrophobic than that of Eo-eRF1bN.

Influence of binding with Eo-eRF3Cm6. Eo-eRF1b and Eo-eRF1bC have been confirmed to bind with Eo-eRF3Cm6 *in vitro*, while Eo-eRF1bN could not bind

with Eo-eRF3Cm6 as shown above. We wanted to determine the effect of this interaction on the structure of Eo-eRF1b and Eo-eRF1bC. Since Eo-eRF3Cm6 has no tryptophan residues, a spectral analysis of the Eo-eRF1b/Eo-eRF3Cm6 complex should reveal conformational changes, if any, from the presence of tryptophans in Eo-eRF1b. In comparing the relative fluorescence profiles of Eo-eRF1b with Eo-eRF1b/Eo-eRF3Cm6, the spectral peak maximum was blue shifted from 340 to 330 nm (Fig. 2). This result suggested that the interaction of the two proteins changed the conformation of Eo-eRF1b at least, although additional structural changes not detected by this analysis may have occurred in Eo-eRF3Cm6 as well. The C-terminal domain of eRF1 is known to interact with the C domain of eRF3. But, comparing the relative fluorescence profiles of Eo-eRF1bC and Eo-eRF1bC/Eo-eRF3Cm6 complex, the spectral peak maximum has no noticeable change (Fig. 2).

Fluorescence quenching measurements. The method of single quenching was used to characterize the local environment of the fluorophores. A polar neutral quencher (acrylamide), anionic quenchers (I^-), and a cationic quencher (Cs^+) were used in this study. The experiments were carried out by monitoring the change in fluorescence intensity at the emission maximum. Both Eo-eRF1bN and Eo-eRF1bC have one tryptophan residue, and their fluorescence changes were plotted according to the Stern–Volmer equation. Eo-eRF1b has two tryptophans, so the fluorescence change was plotted according to a modified Stern–Volmer equation, from which the quenching constant and the fraction of accessible tryptophan residues can be calculated. Typical quenching data for Eo-eRF1b and its domains are given in Table 1. Typical quenching data of the heterodimeric complexes are shown in Table 2. The linearly dependent coefficient R^2 is listed in Tables 1 and 2.

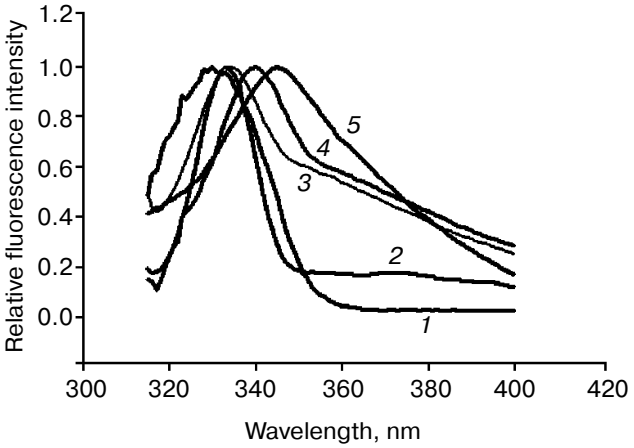

Fig. 2. Fluorescence spectroscopy of Eo-eRF1b, Eo-eRF1bN, and Eo-eRF1bC and their complexes with Eo-eRF3Cm6: *1*) Eo-eRF1b/Eo-eRF3Cm6; *2*) Eo-eRF1bC/Eo-eRF3Cm6; *3*) Eo-eRF1bC; *4*) Eo-eRF1b; *5*) Eo-eRF1bN. The protein concentration was 0.05 mM. The experiments were carried out in 50 mM Tris-HCl, pH 8.0, 50 mM NaCl.

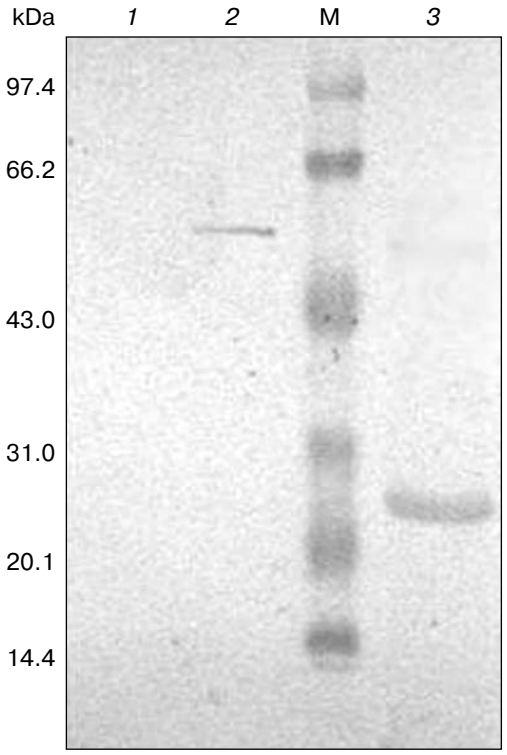

Fig. 1. Pull-down analysis of Eo-eRF1b domains binding with Eo-eRF3Cm6. Western-blot of Eo-eRF1b using anti-His antibody and peroxidase-conjugated goat anti-mouse IgG. M, prestained protein ladder. Lanes: *1*) Eo-eRF1b N binding to Eo-eRF3Cm6; *2*) Eo-eRF1b binding to Eo-eRF3Cm6; *3*) Eo-eRF1bC binding to Eo-eRF3Cm6.

For Eo-eRF1bN, the quenching constant K_{SV} of iodide is far greater than that of the others quenchers. Iodide has negative charge, and this indicates that the tryptophan is located in an area with significant positive charge. For Eo-eRF1bC, the quenching constant K_{SV} of acrylamide is far smaller than that of the others quenchers. So the tryptophan is located in a hydrophobic area.

Eo-eRF1b and Eo-eRF1bC can bind with Eo-eRF3Cm6, while Eo-eRF1bN cannot (Fig. 1). There was little difference between the heterodimeric complex and corresponding Eo-eRF1bC alone; that is, binding with Eo-eRF3Cm6 did not change the quenching characteristic of Eo-eRF1bC by acrylamide. But the quenching characteristic of Eo-eRF1b changed when bound with Eo-eRF3Cm6 (Table 2).

DISCUSSION

Eo-eRF3Cm6 was thought to be the smallest polypeptide to bind with Eo-eRF1a [21]. In our work the

Table 1. Typical quenching data for Eo-eRF1b and its N or C domain

Protein	Quencher	$K_{SV}(M^{-1})$	f_a	R^2
Eo-eRF1bN	acrylamide	9.34		0.9956
	Cs^+	9.66		0.9923
	I^-	91.28		0.9957
Eo-eRF1bC	acrylamide	7.42		0.9928
	Cs^+	44.31		0.9983
	I^-	32.50		0.9946
Eo-eRF1b	acrylamide	8.56	0.822	0.9940
	Cs^+	41.72	0.734	0.9979
	I^-	65.25	0.196	0.9962

Table 2. Typical quenching data for the Eo-eRF1b heterodimeric complexes

Complex	Quencher	$K_{SV}(M^{-1})$	f_a	R^2
Eo-eRF1bC/Eo-eRF3Cm6	acrylamide	8.1		0.9961
	Cs^+	42.6		0.9928
	I^-	31.6		0.9962
Eo-eRF1b/Eo-eRF3Cm6	acrylamide	5.2	0.625	0.9923
	Cs^+	22.1	0.251	0.9981
	I^-	36.5	0.134	0.9955

interaction between Eo-eRF1b and Eo-eRF3Cm6 is confirmed. The conformational changes were detected by comparing the quenching data from Eo-eRF1b and Eo-eRF1b/Eo-eRF3Cm6 heterodimeric complexes. Binding with Eo-eRF3Cm6 caused the fluorescence maximum of Eo-eRF1b to shift from 340 to 330 nm (Fig. 2). At the same time, the quenching parameters of the components also changed. For example, the accessible fraction α of Eo-eRF1b to acrylamide decreased from 0.822 to 0.625, while the quenching constant K_{SV} changed from 8.1 to 5.2. Also, the accessible fraction α and the quenching constant K_{SV} by Ca^+ and I^- were reduced. These results suggest that the fluorophores in Eo-eRF1b/Eo-eRF3Cm6 relocated to a more hydrophobic environment, and the conformation of Eo-eRF1b was driven by this binding.

It is well known that the C-terminal domain of eRF1 interacts with the C domain of eRF3 [8-11]. There is only one tryptophan in Eo-eRF1bC, and a similar fluorescence maximum of Eo-eRF1bC/Eo-eRF3Cm6 complex blue shifting was expected. But, comparing the relative fluorescence profiles of Eo-eRF1bC and Eo-eRF1bC/Eo-eRF3Cm6 complex, the spectral peak maximum has no noticeable change (Fig. 2). So, when binding with Eo-eRF3Cm6, the change in the spectral peak maximum of Eo-eRF1b was not due to this interaction directly. It had been proved that the eRF1 N domain cannot interact with the C domain using isothermal titration calorimetry *in vitro* [14]. And our results by pull-down and Western blot assays are consistent with this conclusion. At the given wavelengths, excitation of Eo-eRF1b resulted in an emission spectrum with a maximum at 340 nm, between that of the Eo-eRF1b N and C domain. When binding with Eo-eRF3Cm6, the spectral peak maximum was blue shifted from 340 to 330 nm, less than that of both the Eo-eRF1b N and C domain (Fig. 2), which indicated that the local environment of the two tryptophans in the Eo-eRF1b N and C domain, respectively, were both made more hydrophobic. Accordingly, the local environment of tryptophans in Eo-eRF1b heterodimeric complex is more hydrophobic than that of Eo-eRF1b and the Eo-eRF1b N and C domains. The reasonable interpretation is that the interaction between the C domain of eRF1b and Eo-eRF3Cm6 induces the N and C domains of Eo-eRF1b to interact with each other. Both the tryptophans in Eo-eRF1b were located on the interface of the eRF1 N and C domains, but there is no evidence show that the two tryptophans in Eo-eRF1b interact with each other. What is more important, the interaction between Eo-eRF1b and Eo-eRF3Cm6 induce a conformational change only in intact Eo-eRF1b. The Eo-eRF1b C domain can interact with Eo-eRF3Cm6, but this interaction could not affect the local environment of the tryptophan in the Eo-eRF1 C domain, while the Eo-

eRF1b N domain cannot interact with Eo-eRF3Cm6. In conclusion, the interaction between Eo-eRF1b N and C domain is driven by the interaction between Eo-eRF1b and Eo-eRF3Cm6.

This work was supported by grants from the National Natural Scientific Foundation of China (No. 31071924) and Natural Sciences Foundation of Shanxi (2010011040-1).

REFERENCES

1. Frolova, L., Le Goff, X., Rasmussen, H. H., Cheperegin, S., Drugeon, G., Kress, M., Arman, I., Haenni, A. L., Celis, J. E., and Philippe, M. (1994) *Nature*, **372**, 701-703.
2. Song, H., Mugnier, P., Das, A. K., Webb, H. M., Evans, D. R., Tuite, M. F., Hemmings, B. A., and Barford, D. (2000) *Cell*, **100**, 311-321.
3. Kim, O. T., Yura, K., Go, N., and Harumoto, T. (2005) *Gene*, **346**, 277-286.
4. Kononenko, A. V., Dembo, K. A., Kiselev, L. L., and Volkov, V. V. (2004) *Mol. Biol. (Moscow)*, **38**, 303-311.
5. Salas-Marco, J., Fan-Minogue, H., Kallmeyer, A. K., Klobutcher, L. A., Farabaugh, P. J., and Bedwell, D. M. (2006) *Mol. Cell Biol.*, **26**, 438-447.
6. Korostelev, A., Zhu, J., Asahara, H., and Noller, H. F. (2010) *EMBO J.*, **29**, 2577-2585.
7. Zavialov, A. V., Mora, L. R., Buckingham, H., and Ehrenberg, M. (2002) *Mol. Cell*, **10**, 789-798.
8. Ebihara, K., and Nakamura, Y. (1999) *RNA*, **5**, 739-750.
9. Eurwilaichitr, L., Graves, F. M., Stansfield, I., and Tuite, M. F. (1999) *Mol. Microbiol.*, **32**, 485-496.
10. Ito, K., Ebihara, K., and Nakamura, Y. (1998) *RNA*, **4**, 958-972.
11. Merkulova, T. I., Frolova, L. Y., Lazar, M., Camonis, J., and Kisselev, L. L. (1999) *FEBS Lett.*, **443**, 41-47.
12. Cheng, Z., Saito, K., Pisarev, A. V., Wada, M., Pisareva, V. P., Pestova, T. V., Gajda, M., Round, A., Kong, C., Lim, M., Nakamura, Y., Svergun, D. I., Ito, K., and Song, H. (2009) *Genes Dev.*, **23**, 1106-1118.
13. Fan-Minogue, H., Du, M., Pisarev, A. V., Kallmeyer, A. K., Salas-Marco, J., Keeling, K. M., Thompson, S. R., Pestova, T. V., and Bedwell, D. M. (2008) *Mol. Cell.*, **30**, 599-609.
14. Kononenko, A. V., Dembo, K. A., Kiselev, L. L., and Volkov, V. V. (2008) *Proteins*, **70**, 388-393.
15. Salas-Marco, J., and Bedwell, D. M. (2004) *Mol. Cell Biol.*, **24**, 7769-7778.
16. Hatin, I., Fabret, C., Rousset, J. P., and Namy, O. (2009) *Nucleic Acids Res.*, **37**, 1789-1798.
17. Liang, A., Brunen-Nieweler, C., Muramatsu, T., Kuchino, Y., Beier, H., and Heckmann, K. (2001) *Gene*, **262**, 161-168.
18. Song, L., Chai, B. F., Wang, W., and Liang, A. H. (2006) *Res. Microbiol.*, **157**, 842-850.
19. Wang, Y., Chai, B. F., Wang, W., and Liang, A. H. (2010) *Biosci. Rep.*, **30**, 425-431.
20. Chavatte, L., Seit-Nebi, A., Dubovaya, V., and Favre, A. (2002) *EMBO J.*, **21**, 5302-5311.
21. Wang, W., Chai, B. F., Heckmann, K., and Liang, A. H. (2004) *Biotechnol. Lett.*, **26**, 959-963.
22. Stobiecka, A. (2005) *J. Photochem. Photobiol.*, **80**, 9-18.
23. Kwaambwa, H. M., and Maikokera, R. (2007) *Colloids Surf. Biointerfaces*, **60**, 213-220.